International Journal of Multidisciplinary Research And Studies

Available online at https://ijmras.com/

INTERNATIONAL JOURNAL OF MULTIDISCIPLINARY RESEARCH AND STUDIES
ISSN: 2640 7272
Volume:03; Issue:05 (2020)

SYSTEMATIC VARIETY OF THE TYPE CREEPING

SAMREEN JAHAN
M.Phil., Roll No.: 142102 Session-2014-15
Department of Zoology, B.R.A. Bihar University, Muzaffarpur, India
E-mail: samshanzasamu@gmail.com

Abstract

The theory that creep is caused by diffusion-like processes, with sediment flow linearly related to surface slope, is supported by observations made on convex hills, which demonstrate that soil thickness decreases with increasing topographic curvature Such movement of individual soil grains could be caused by burrowing creatures (such as worms, ants, and gophers) and by tree throw (trees that have been uprooted, typically by high winds, often carry soil and bedrock attached to the root wad), coupled with localized slope wash; however, field observations and laboratory studies show that nondiffusive processes, such as shear and depth-dependent viscous-like flow, may also occur. Burrowing creatures are examples of such organism. In addition, the observed connections between soil depth and slope curvature on linear and compound slopes are not consistent with a straightforward linear relationship between sediment flow and surface slope alone.

keywords: Systematic, Variety, Creeping

Introduction

Soils on slopes are often formed as a result of the weathering and subsequent disintegration of the bedrock below (Carson and Kirkby, 1972; Dietrich et al., 1995; Heimsath et al., 1997). On steep terrain, the most common kind of soil erosion is likely to be landslides; however,

creep and slope wash are also important factors in the movement of dirt downwards. The theory that creep is caused by diffusion-like processes, with sediment flow linearly related to surface slope, is supported by observations made on convex hills, which demonstrate that soil thickness decreases with increasing topographic curvature Such movement of individual soil grains could be caused by burrowing creatures (such as worms, ants, and gophers) and by tree throw (trees that have been uprooted, typically by high winds, often carry soil and bedrock attached to the root wad), coupled with localized slope wash; however, field observations and laboratory studies show that nondiffusive processes, such as shear and depth-dependent viscous-like flow, may also occur. Burrowing creatures are examples of such organism. In addition, the observed connections between soil depth and slope curvature on linear and compound slopes are not consistent with a straightforward linear relationship between sediment flow and surface slope alone. Estimating creep processes has been done using rods, blocks, and flexible tubes that have been put into the soil (Fleming and Johnson, 1975; Young, 1960). However, these methods are too cumbersome to analyze grainscale sediment movement, which necessitates the use of tagged particles (Selby, 1993). It would be a tremendous operation to insert tagged grains into a dirt mantle and then identify those grains using microscale positional measurements. If, on the other hand, the grains that are brought to the surface by bioturbation and tree throw are subsequently buried, then the amount of vertical mixing that occurs at the grain scale can be determined by measuring the amount of time that has passed since individual soil grains were last at the surface. Single-grain optical dating was used to accomplish this, and it is based on an optically stimulated luminescence (OSL) signal that accumulates within buried quartz grains (below a few millimeters of the surface) and is reset to zero by exposure to sunlight. This allowed us to determine the age of the quartz grains in question.

The transport mechanisms determine the optical ages of grains found at various levels. For example, grains moving through a surface layer would be occasionally exposed to sunlight, but granules never exposed at the surface should have "infinite" ages. Alternately, if the whole soil column were to be mixed together, the result would be grains of varying ages from the top of the soil to the bottom. Every movement of a soil grain that occurs downhill may be resolved into two components: slope normal and slope parallel. The slope-normal velocity of a grain is the only thing that can be deduced from the optical age of a grain. We are unable to determine the slope-parallel velocity of individual grains; however, it is possible to compute the depth-averaged velocity provided the rate of soil production from rock weathering is known at each site. The soil-production rates at our research site were previously established from

measurements of the in situ cosmogenic nuclides 10Be and 26Al (Heimsath et al., 2000). These soil-production rates are employed in a novel method to calculate slope-parallel velocities here. In addition, modeling of the landscape development of the site (Braun et al., 2001) brought to light the need for a more in-depth knowledge in the area of the sediment transport mechanisms that are active on soil-mantled landscapes.

It is generally accepted that the presence of earthquake repeaters, which are co-located seismic events of comparable magnitude with highly similar waveforms breaking the same fault patch with an almost identical mechanism, is an indication that the fault surrounding the earthquake asperity is (aseismically) creeping. Repeaters are defined as co-located seismic events breaking the same fault patch with an almost identical mechanism. Repeating earthquakes may take place either during periods of transitory stress, such as the afterslip that follows big earthquakes, or during periods of permanent tectonic loading along tectonic faults. Within the scope of our research, we focus on the latter. The Main Marmara Fault (MMF), which is located near to the population center of Istanbul below the Marmara Sea, is a section of the western portion of the North Anatolian Fault Zone (NAFZ), which separates the Anatolian and Eurasian plates. It is also known as the Main Marmara Fault. Although the main NAFZ branches to the east and west of the MMF ruptured in earthquakes with a magnitude greater than seven in the past century, the MMF itself is considered to be a seismic gap that has the potential to host an earthquake with a magnitude greater than seven in the not too distant future.

It is essential to have an accurate understanding of the degree of aseismic creep of the off-shore MMF strand in order to perform a more accurate seismic hazard assessment for the city of Istanbul, however this topic is the subject of much controversy. We study a newly produced seismicity inventory of the Sea of Marmara for repeated occurrences throughout the whole MMF, building on previous research that detected recurring earthquakes in the western portion of the MMF. The collection covers the years 2006-2020, including about 14,000 occurrences with magnitudes ranging from M0.3 to M5.7, and was constructed using data from regional permanent stations that are administered by both AFAD and KOERI. A two-step technique was used to automatically choose the timings of the phase onsets. This procedure made use of higher-order statistics and an AIC-representation of the waveforms to provide a coarse and fine-tuned estimate of the P and S onsets, respectively.

In order to acquire the final hypocenters, the obtained onset-times were input into the Octree localization algorithm of the probabilistic NLLoc program. This technique was combined with

a regional velocity model and station adjustments. In order to find repeating earthquakes, we first partition the MMF into overlapping segments and then do a station-wise cross-correlation analysis for all accessible event waveforms in each segment. This allows us to search for repeating earthquakes. Waveforms that are correlated with one another begin one second before the P-wave arrives and encompass the whole waveform, including the coda for the S-wave. Waveforms were bandpass filtered between 2 and 20 Hz so that the frequency spectrum could be preserved in relatively high resolution. We apply stringent selection criteria and only consider aftershock sequences or earthquake swarms to have repeating events if they have a normalized cross-correlation coefficient that is greater than 0.9 at at least three stations and a temporal separation of more than 30 days.

This allows us to exclude bursts of highly similar events that can occur during aftershock sequences or earthquake swarms. The highest concentration of repeating earthquakes is located below the western Marmara Sea (Central Basin and Western High), with a systematic decrease of repeaters towards the east (Kumburgaz Basin), and none at all in the presumably locked Princess Islands section of the MMF immediately south of Istanbul. This area of the Marmara Megathrust Fault (MMF) is thought to be locked. These data, for the first time, present a consistent view of the degree of creep over the whole overdue Marmara region of the NAFZ. This image was acquired from permanent onshore stations, and it refined prior results obtained from specific sites utilizing local seabed deployments.

OBJECTIVES

1. Ground cover: One of the primary objectives of using creeping plants is to provide ground cover, particularly in areas where grass may not grow well or may be difficult to maintain. Creeping plants can be used to cover bare patches of soil, prevent soil erosion, and create a lush, green landscape.

2. Soil stabilization: Creeping plants can also be used to stabilize slopes and prevent soil erosion. By spreading horizontally across the ground, creeping plants can help to hold soil in place and prevent runoff.

RESEARCH METHODOLOGY

The first step in the study was a systematic literature search. For this purpose, journal and conference articles dealing with the creep behavior of SFRC and PFRC, on material and structural levels, were considered. For the literature search, the online databases of Scopus and Web of Science were used, complemented with personal archives compiled previously. The following search terms were used for Article Titles in Scopus and Web of Science:

1. "fib** reinforced concrete" AND "long-term"
2. "fib** reinforced concrete" AND "time-dependent"
3. "fib** reinforced concrete" AND "creep"
4. "synthetic" AND "fib**" AND "creep"
5. "polypropylene" AND "fib**" AND "creep"

The syntax "fib" was used to cover both British and American English spelling (fibre vs. fiber). Search terms 1–3 were used to find research at the concrete specimen and structural member level, whereas search terms 4–5 were used to find on research on the single fiber or fiber material level (focusing on "synthetic/polymeric" fibers as these are more prone to undergo creep and polypropylene fibers as the most widely used among this type of fiber). The initial search yielded a total of 250 studies: 125 on Scopus, 83 on Web of Science and 42 from the personal archive of the researchers. The next step was the removal of duplicate studies which led to the removal of 90 studies, leaving a total of 160 distinct journal and conference articles.

The remaining articles were screened for language (only studies in English were retained) and topic (only studies on concrete and time-dependent behavior were retained—studies on, e.g., asphalts, fiber composites and durability were excluded). This led to the removal of 69 studies, leaving 91 studies in the database. Finally, through the institutional access available to the researchers, 19 studies could not be accessed. Therefore, the final number of studies considered in the review was 72. These studies were divided into three groups: (1) fiber level, (2) concrete level, and (3) structural level. When dividing the studies according to their content, certain studies were categorized into more than one group. Therefore, the 70 studies were divided into (overlapping) groups of 10, 43, and 23 studies for groups (1), (2), and (3), respectively, summarized in Table 1.

Table 1 Summary Of Systematic Literature Search

Topic/Group	No. of Studies/References
Total no. of studies	72; [26,28,34–103]
Fiber level	10; [28,34–42]
Concrete level	43; [28,37,43–83]
Structural level	23; [26,44,45,84–103]

Any systematic review introduces a certain bias. Herein, the bias consists in several factors. First, the selection of studies only in English potentially excludes a body of knowledge in other languages. However, considering that the large majority of studies indexed in Scopus and Web of Science are in English, this bias is considered not significant. Second, only journal and conference articles are considered, and documents such as reports and theses are excluded. This bias can also be considered negligible as the number of these documents is not large, and, e.g., doctoral theses are typically accompanied by journal publications of the same content. Finally, a certain bias is introduced by the databases themselves; however, as the most renowned and accepted databases, Scopus and Web of Science were considered appropriate.

DATA ANALYSIS

As with other properties of concrete, the long-term behavior of FRC observed on the material level cannot be directly extrapolated to structural behavior. Therefore, full scale long-term tests on FRC members are necessary. However, executing such tests is a challenge due to the large numbers of parameters involved, their time-consuming nature, and significant economic cost.

Fig. 1 Experimental Setup For Testing Frc Beams (Authorized Reprint From)

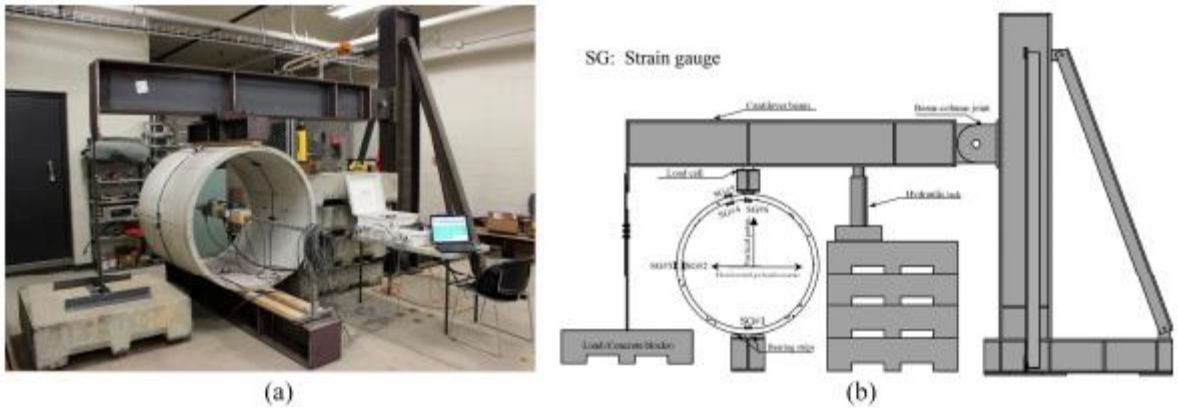

Fig. 2 (A) Photograph And (B) Schematic Diagram Of The Long-Term Test Setup

While there are not enough results for analyzing in detail the effect of certain parameters, several important general conclusions can be drawn. First, it can be seen that material-level behavior does not translate to structural behavior, particularly in the case of PFRC members without steel reinforcement in the studies by Park et al. and Attiogbe et al. the tested pipes did not exhibit drastic increases of vertical displacements, nor creep failure, rather, a very minor effect of pre-cracking on the long-term vertical displacements was found (both for buried and unburied pipes). Secondly, in the case of R-SFRC members, the steel fibers always decreased deflections and crack widths. For example, Tan et al. found that after 10 years, deflections of R-SFRC beams with 2% of steel fibers were 36% smaller than the deflections of RC beams. Nakov et al. saw decreases in total deflections after one year of 18% and 25% for R-SFRC with 0.8% and 1.6% of steel fibers, respectively, relative to RC. In the study by Aslani et al. deflections always decreased with the addition of fibers (~0.5%). Adding only steel fibers was the most effective, followed by mixing steel and polypropylene fibers in equal volumes, whereas adding polypropylene fibers decreased deflections only slightly; nonetheless, all beams experienced deflection stabilization after 240 days. At the same time, results for crack widths are not conclusive for R-SFRC, although generally crack widths tend to be reduced relative to RC. It should be noted that the majority of the "hybrid-FRC" members (i.e., members with fibers and steel reinforcement) had relatively large reinforcement ratios. It is possible that long-term deflection and crack development will be more critical for members containing fibers and minimum steel reinforcement; therefore, this is something that should be determined in future research. Nonetheless, it can be safely claimed that creep failure of FRC elements in the presence of minimum steel reinforcement is not to be expected.

SERVICEABILITY LIMIT STATE (SLS) DESIGN OF FRC

Plizzari and Serna specify two types of FRC structural applications: “enhancing crack behavior which is particularly important at SLS and also for durability requirements” and “replacing all or part of the conventional reinforcement for structural capacity at Ultimate Limit States (ULS)”. In practice and in cases where cracking is expected under service conditions, hybrid-FRC members are most likely to be used (with fibers and steel reinforcement). Whether fibers are added only for enhancing SLS behavior or whether steel reinforcement is partially replaced, in order to assess deflections and crack widths, the creep behavior of FRC needs to be considered.

Because of the significant uncertainties still related with FRC in general, and its creep behavior in particular, codes tend to apply strict limitations on its properties when it is to be used as a structural material. For example, the fib Model Code 2010 requires a minimum “performance class” of “1.0 a” when FRC residual strength is required for equilibrium conditions (complete or even partial reinforcement substitution): the minimum values of f_{R1k} and f_{R3k} (characteristic residual strengths obtained in the EN 14,651 test at a CMOD of 0.5 and 2.5 mm, respectively) are 1.0, and 0.5 MPa, respectively. Furthermore, f_{R1k} must be greater than $0.4 \cdot f_{Lk}$, where f_{Lk} is the characteristic limit of proportionality as defined by EN 14,651 [112]) and f_{R3k} must be greater than $0.5 \cdot f_{R1k}$. In terms of ductility, the fib Model Code 2010 also requires one of the following conditions to be satisfied:

where δ_u is the ultimate displacement of the structure or member, δ_{peak} is the displacement at peak load, and δ_{SLS} is the displacement under service conditions. In reality, these conditions are very strict, and usually either preclude the use of FRC without reinforcement or require flexural hardening of the structural element. However, besides these general recommendations, there is not much guidance in the fib Model Code 2010, or other codes (for example the Spanish EHE-08, in terms of providing specific models or expressions for incorporating creep behavior of FRC into structural analysis and design. Even though certain research in this direction has been conducted and some models have been put forward, currently this area remains the one that is most open to advances. One of the earliest works in this area was done by Tan et al. and continued by Tan and Saha .

The authors formulated an adjustment of the ACI 318 Building Code procedure for deflection control making it applicable to SFRC beams, mostly based on own experimental results. The ACI 318 model is based on calculating deflections using an effective moment of inertia

(interpolated between the uncracked and fully cracked states). Instantaneous deflections are multiplied by a factor to take into account creep, whereas deflections due to shrinkage are calculated from the induced curvature. In terms of SFRC adjustments, the proposed method provides an expression for the moment of inertia of a cracked section, considering the contribution of fibers through a ratio of the moduli of elasticity of steel fibers and concrete and the equivalent areas of fibers in the compressed and tensile zone.

At the level of deflections, the multiplicator for creep effects is adjusted by an empirical formula based only on the volume of steel fibers Vf . These authors also propose obtaining SFRC crack widths by adjusting those calculated for RC members through a linear relation dependent also on the fiber volume Vf . Relatively good agreement of model predictions with results of 10-year beam measurements was found. Since the method was developed on own experimental results, there is room for improvement and generalization of the method by including properties such as tensile creep of FRC.

So far, most work on SLS constitutive modeling and design of SFRC has been undertaken in a sequence of papers by Amin and Gilbert, Amin et al., and Watts et al. The authors started by developing a model for the tension stiffening effect in R-SFRC and then succeeded in applying the model in the calculation of instantaneous crack widths and instantaneous and time-dependent deflections . Amin et al. proposed an extension of the so-called tension chord model (TCM) to R-SFRC to model the tension stiffening effect, also explicitly accounting for shrinkage. A general scheme of the model is reproduced in Figure 10, where λ is a factor between 0 and 1, f ct is the concrete tensile strength, sr is the crack spacing, w is the crack width, σf is the stress in steel fibers crossing a crack, σc,avg is the average tension-stiffening stress, σs,cr is the steel reinforcement stress in the cracked section, Materials σs,avg is the average stress in steel reinforcement, and 2020, 13, x FOR PEER REVIEW τb is the bond stress.

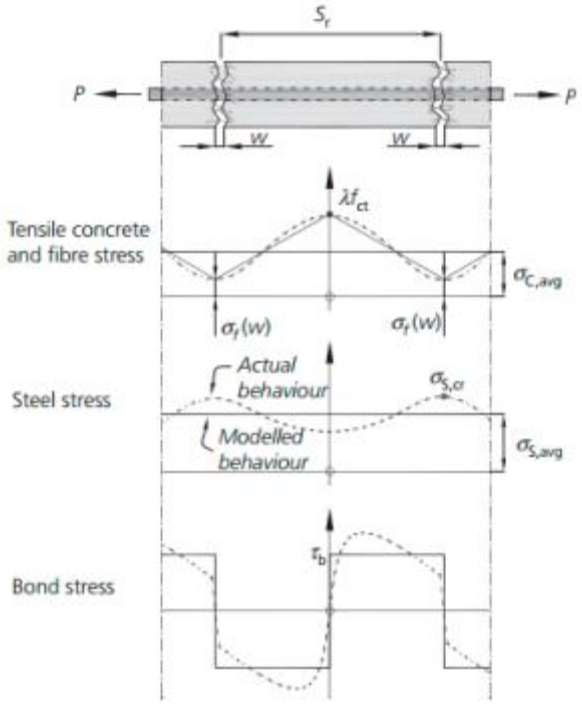

Fig. 3 Tension Chord Including The Effect Of Steel Fibers And Reinforcing Bar (Authorized Reprint From)

The proposed model allowed these authors to define tension stiffening stresses for minimum and maximum crack spacing scenarios. The results were verified against own experimental results as well as those previously published in literature. Subsequently, Amin et al. applied the TCM model for R-SFRC to calculating instantaneos deflections of members in bending. They built on the model originally proposed by Kenel et al. In this model, deflections are not calculating by interpolating between deflections calculated for the uncracked and fully cracked states—as is done in the fib Model Code 2010 approach —but rather by calculating the deflection of a fully cracked member and reducing it by tension stiffening contributions:

where a is the total deflection, a1 is the deflection of the member that would be obtained assuming it is fully cracked over its entire length, and Δa0 and Δa1 are the stiffening effects of uncracked and cracked regions of the member, respectively. The stiffening effects are due to a "curvature offset" $\Delta\chi$ for which the Amin et al. propose a formulation for R-SFRC (based on their TCM model), as well as a method of calculating cracked sectional properties, similar to the method applied by Tan et al. The method was successfully verified using available experimental data. Watts et al. further applied this model to time-dependent deflections of R-SFRC members. The model is based on Equation (7) and the previous study by Amin et al., expanded by accounting for the increases in curvature over time due to creep (only compressive

creep is considered) and shrinkage. A comparison with available test data showed good results. Finally, based on the same TCM model Amin and Gilbert proposed an iterative procedure for instantaneous crack width calculation. It can be seen that, although current codes still do not incorporate provisions for time-dependent analysis of FRC, progress is being made. The TCM model developed by Amin et al. is a significant way forward. What still remains is the adaptation of the model to PFRC on the tension chord level, as well as the incorporation of time-dependent polymeric fiber properties into long-term deflection predictions. This can potentially be done by modifying sectional properties as is achieved by the effective modulus method and the compressive creep coefficient. The previous sections have shown that research on the creep behavior of FRC exists on the structural level, both in terms of experimental and theoretical work. However, the body of literature is still insufficient for design and practical purposes and more work is needed until it is mature enough to translate into design codes and wider practical applications by industry. In terms of experimental research, work should be focused on hybrid-FRC but also on cases with reinforcement ratios close to the minimum; particularly, more experiments are needed on R-PFRC. Furthermore, the current experiments do not provide a clear link between long-term bending or uniaxial tension tests on the material and structural level, i.e., available results on the material level (e.g., crack width creep coefficients) are not applicable to structural tests. In terms of theoretical work, the broadening of current models (whether existing ACI or fib Model Code approaches or TCM models) to R-PFRC is still lacking. Current results from numerical simulations are reason for optimism that with more comprehensive testing, formulation, validation, and calibration of theoretical models through numerical parametric studies will be possible.

CONCLUSION

A comprehensive and analytical literature review on the creep behavior of FRC and FRC structural members has been offered in this research. The creep behavior of FRC and FRC structural members was investigated. The research included both experimental and theoretical studies, and it encompassed research on the single fiber level, the material level of FRC, and the structural level of FRC and hybrid-FRC member structures. The approach that was used for literature search and filtering is described in an open and honest manner, and any possible biases are spoken about (only literature written in English as well as journal and conference papers were taken into consideration). In spite of the review that was carried out in this article, this provides a number of significant findings drawn from the most recent state of the art as well as clear suggestions for research that should be conducted in the future. On the level of

the single fiber, the results of single fiber creep tests allow one to draw the conclusion that SFRC might be susceptible to pull-out creep, whereas PFRC is susceptible to fiber creep as well, provided that the fibers are subjected to permanent tensile stresses of magnitudes that are incompatible with the temperature- and time-dependent mechanical properties of each type of polymeric fibers. Series While Kelvin chain models are capable of describing the creep behavior of both SFRC and PFRC, more study is required before a unified model that is applicable to both forms of FRC can be proposed. At the level of the FRC material, there is still a significant amount of variation in the ranges of parameter values that are used in long-term uniaxial stress and bending testing. In the future, testing should involve not just bending or tension on a single axis for a prolonged period of time, but also shrinkage and compressive creep.

REFERENCES

1. Di Prisco, M.; Plizzari, G.; Vandewalle, L. Fibre reinforced concrete: New design perspectives. Mater. Struct. 2009, 42, 1261–1281.

2. FIB Bulletin 83. In Precast Tunnel Segments in Fibre-Reinforced Concrete; International Federation for Structural Concrete (fib): Lausanne, Switzerland, 2018.

3. De la Fuente, A.; Blanco, A.; Armengou, J.; Aguado, A. Sustainability based-approach to determine the concrete type and reinforcement configuration of TBM tunnels linings. Case study: Extension line to Barcelona Airport T1. Tunn. Undergr. Space Technol. 2017, 61, 179–188.

4. De La Fuente, A.; Casanovas-Rubio, M.D.M.; Pons, O.; Armengou, J. Sustainability of Column-Supported RC Slabs: Fiber Reinforcement as an Alternative. J. Constr. Eng. Manag. 2019, 145, 04019042.

5. WBCSD. The Cement Sustainability Initiative. World Bus. Counc. Sustain. Dev. 2017, 41. Available online: https://docs.wbcsd.org/2009/07/CSI-RecyclingConcrete-FullReport.pdf (accessed on 12 October 2020).

6. Scrivener, K.L.; Vanderley, J.M.; Gartner, E.M. Eco-Efficient Cements: Potential, Economically Viable Solutions for a Low-CO2 , Cement Based Materials Industry; UN Environment: Paris, France, 2016.

7. Roesler, J.R.; Altoubat, S.A.; Lange, D.A.; Rieder, K.A.; Ulreich, G.R. Effect of synthetic fibers on structural behavior of concrete slabs-on-ground. ACI Mater. J. 2006, 103, 3–10.

8. Meda, A.; Plizzari, G.A.; Riva, P. Fracture behavior of SFRC slabs on grade. Mater. Struct. Constr. 2004, 37, 405–411.

9. Alani, A.M.; Beckett, D. Mechanical properties of a large scale synthetic fibre reinforced concrete ground slab. Constr. Build. Mater. 2013, 41, 335–344.

10. Meda, A.; Plizzari, G.A. New design approach for steel fiber-reinforced concrete slabs-on-ground based on fracture mechanics. ACI Struct. J. 2004, 101, 298–303.

11. Chen, S. Steel fiber concrete slabs on ground: A structural matter. ACI Struct. J. 2007, 104, 373–375.

12. Caratelli, A.; Meda, A.; Rinaldi, Z.; Romualdi, P. Structural behaviour of precast tunnel segments in fiber reinforced concrete. Tunn. Undergr. Space Technol. 2011, 26, 284–291.